



ELSEVIER

Tectonophysics 264 (1996) 295–307

TECTONOPHYSICS

Vertical seismic profile results from the Kola Superdeep Borehole, Russia

B.J. Carr^{a,*}, S.B. Smithson^a, N. Kareav^b, A. Ronin^b, V. Garipov^c, Y. Kristofferson^d,
P. Digranes^d, D. Smythe^e, C. Gillen^f

^a Department of Geology and Geophysics, University of Wyoming, Laramie, WY 82071-3006, USA

^b V.I.R.G., 20 Fajansovaja, 193019 St. Petersburg, Russia

^c Russian State Committee on Geology, 4–6 B Gruzinskaya, 123242 Moscow, Russia

^d Institute of Solid Earth Physics, University of Bergen, Allegt. 41, 5007Bergen, Norway

^e Geology and Applied Geology, University of Glasgow, Glasgow G12 8QQ, UK

^f University of Edinburgh, 11 Buccleuch Place, Edinburgh EH8 9LW, UK

Received 28 February 1995; accepted 30 January 1996

Abstract

Multi-offset vertical seismic profiles (VSPs) from the Kola Superdeep Borehole (SG-3), as part of a larger seismic study of the Kola region conducted during the spring of 1992, sample the dipping Pechenga complex from 2175 m to 6000 m and contribute to the understanding of reflectivity in crystalline and Precambrian environments. From the surface to 6000 m, the SG-3 borehole penetrates interlayered Proterozoic metavolcanic and metasedimentary units and a mylonitic shear zone ranging from greenschist to amphibolite metamorphic grade, respectively. The Kola VSPs display a 6% velocity decrease which coincides to a mylonitic shear zone located between 4500 m and 5100 m within the SG-3 borehole. Seismic interfaces are identified by mode-converted energy (PS, and SP transmissions and reflections) in addition to primary seismic phases. The VSP shear wave energy is generated at or near the source by vertical vibrators. P-wave and S-wave reflections are generally detected from the same reflecting horizons, but increases in relative S-wave and SP reflection amplitudes originate at 1900 m, 3800 m, 4500 m, and 5100 m depths. These depths coincide with zones of elevated V_p/V_s and may support the presence of free pore fluid which is reported from initial drilling. For the Proterozoic lithologies sampled by the VSP, reflection events result from five mylonitic shear zones and three lithologic contrasts.

Keywords: vertical seismic profiling; Kola Superdeep Borehole; reflectivity; crystalline; mode-converted; crystalline pore fluids

1. Introduction

The nature of seismic reflectivity in crystalline rocks has been a dominating question in crustal seis-

mology for many years (e.g., Steinhart and Meyer, 1961; Fuchs, 1969; Smithson et al., 1977; Hale and Thompson, 1982; Blundell and Raynaud, 1986; Fountain et al., 1987; Valasek et al., 1989; Smithson and Johnson, 1989; Pavlenkova, 1991; Mooney and Meissner, 1992; Fountain et al., 1994; Levander et al., 1994). Until recently, borehole measurements of the seismic wavefield recorded at standard sig-

* Corresponding author. Present address: Oak Ridge Natinal Lab, Environmental Sciences Division, P.O. Box, MS-6400, Oak Ridge, TN 37830-6400, USA. Fax: +1 423 574-7420.

nal frequency bandwidths have been rare in crystalline lithologies. Scientific boreholes such as the Kola Superdeep Borehole (Koslovsky, 1987), KTB deep drilling project in Germany (Hohrath et al., 1992; Söllner et al., 1992; Lüschen et al., 1996), Gravberg-Siljan (Juhlin and Windhofer, 1988), and Cajon Pass (Rector, 1988) provide the primary calibration available for crustal surface seismic profiles in crystalline sequences. To add further information about the reflectivity in Precambrian rocks, the Universities of Wyoming, Bergen, and Glasgow, with colleagues from the Russian State Committee on Geology and the Institute of Physics of the Earth of the Academy of Sciences, Moscow, conducted seismic data acquisition in and around the Kola Superdeep Borehole (SG-3) in 1992. The purpose of this paper is to discuss results obtained from the recorded VSPs.

The Kola multi-offset VSPs will illustrate how lithology, structural setting, and anisotropy affect the seismic wavefield. At Kola, VSPs sample the Proterozoic Pechenga series metavolcanic and metasedimentary rocks from depths of 25–500 m and 2175–6000 m at 25-m increments. The Pechenga rocks display metamorphism from prehnite–pumpellyite facies (<1700 m depth) to greenschist facies (1700–4500 m depth), and epidote–amphibolite facies (4500–6000 m depth). From 4340 m to 5100 m depth in the SG-3 borehole, a mylonitic shear zone (known as the Luchlompol fault zone) separates the greenschist and epidote–amphibolite facies units.

In addition to the 1992 Kola VSPs, this analysis incorporates Russian multi-component VSP data collected from the depths of 1120–2000 m with source offsets and azimuths coinciding to the 1992 data. The additional VSP data were recorded at 20-m

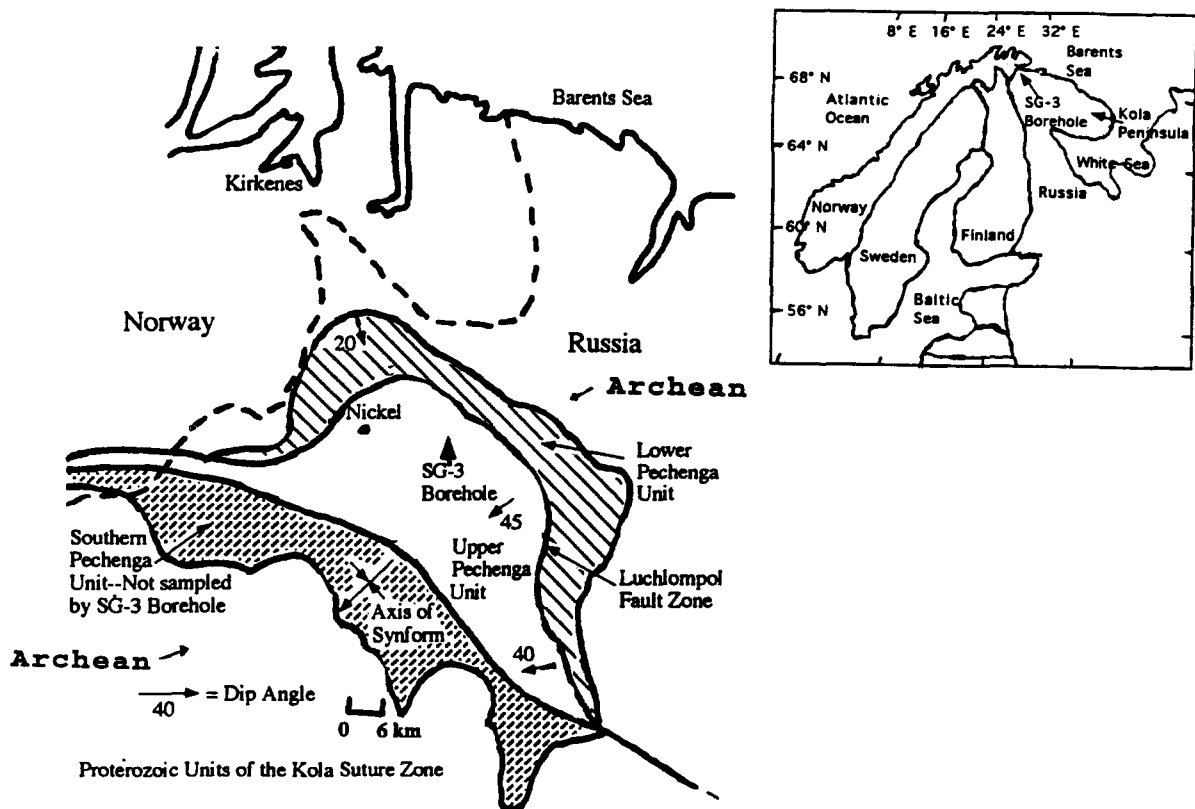


Fig. 1. Location of the SG-3 borehole (top), and schematic of the SG-3 borehole location within the Kola suture zone (bottom). Selected tectonic and structural features of the Kola suture zone are also indicated (modified from Berthelsen and Marker, 1986).

increments with an explosive source. These records were corrected to zero-phase before inclusion to assure that the two data sets are comparable.

The combined Kola VSPs allow us to identify the depths and causes of reflectivity, and speculate on the existence of free pore fluid and subhorizontal reflectivity (detected in surface seismic data) in the SG-3 vicinity. Seismic anisotropy and deeper reflections are also detected in these VSPs but will be discussed in future publications.

2. Geology and reflectivity of the Kola Borehole

The SG-3 borehole is drilled to 12 km within the Precambrian crust of the NE Baltic Shield (Fig. 1) and passes through 6800 m of Proterozoic rocks continuing to 12 km in Archean rocks. The Pechenga

complex is a plunging synform where the layers dip 20–50° to the southwest and represents a 1.9 Ga arc-continent and subsequent continent–continent suture zone (Berthelsen and Marker, 1986). The SG-3 borehole site lies close to the plunge axis of this structure (Fig. 1). The Proterozoic lithologies can be divided into three basic tectonic units which are: (1) upper Pechenga unit (0–4500 m); (2) Luchlompol fault zone (4500–5100 m); and (3) Lower Pechenga unit (5100–6800 m). The details of the Pechenga sequences will be emphasized in this paper since the 1992 VSP recording concluded at 6000 m due to a blockage at this depth.

The upper Pechenga unit consists of Proterozoic age tholeiitic basalts with a significant amount of clastics and gabbro diabase intrusives at either prehnite–pumpellyite or greenschist facies (Fig. 2).

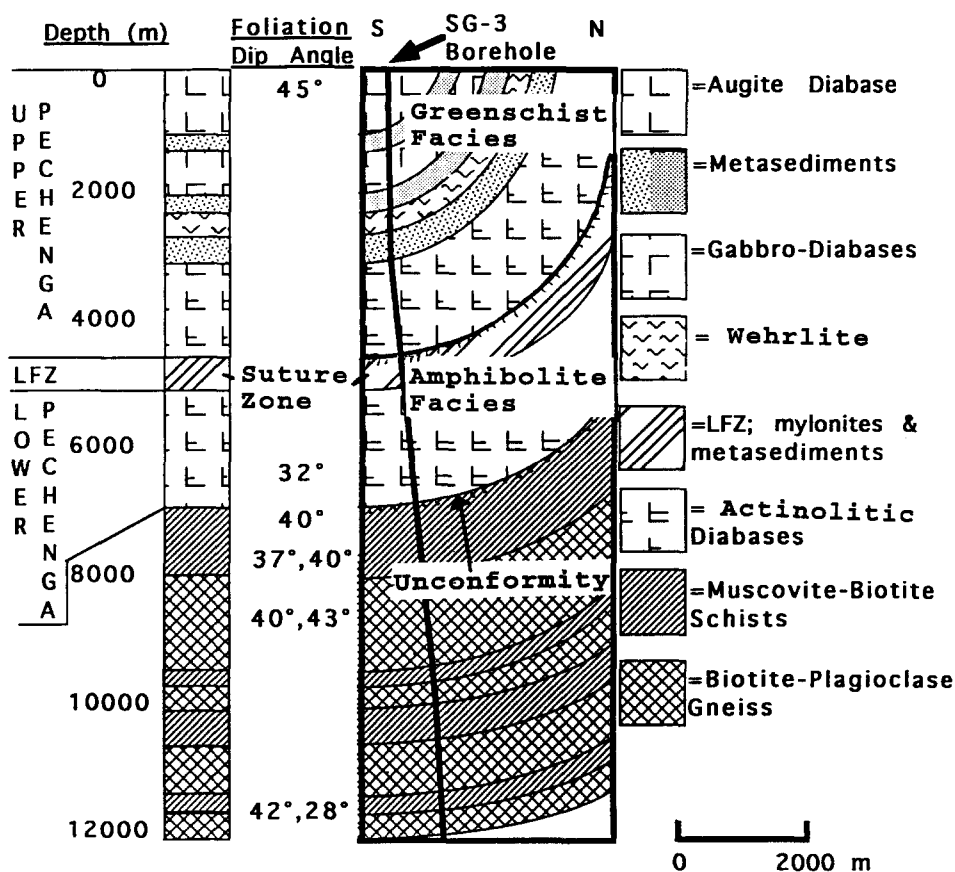


Fig. 2. Generalized stratigraphic section for the Kola Superdeep Borehole, modified after Lanev et al. (1987). LFZ = the Luchlompol fault zone. Foliation dips are taken from core samples reported by Vernik et al., 1994.

This unit is also characterized by the highest densities (2.88–3.0 g cm⁻³), highest P-wave velocities (6.4–6.6 km/s), low porosity, and low permeability (Pavlenkova, 1991). The layered metasedimentary units range from breccia/sandstones to siltstones/phyllites. The sedimentary zone is interrupted by zones of tuffaceous rocks and diabase sheets. Synthetic seismograms (1-D) generated from a wireline sonic log provide an opportunity to study the theoretical reflectivity of these Proterozoic sequences (Fig. 3). The synthetic seismogram was created with

a 45 Hz zero-phase Ricker wavelet (to simulate the average frequency of the 1992 data) and assumes a vertically incident source with infinitely extending interfaces. In the upper Pechenga unit, reflectivity is generated at depths corresponding to contacts between gabbro and phyllite (A), gabbro and sandstone (B), and gabbro and tuffs (C, C*) (Fig. 3). Clearly, the metasedimentary sequences between 1059 and 2805 m provide abundant acoustic impedance contrasts and the majority of reflections within this interval.

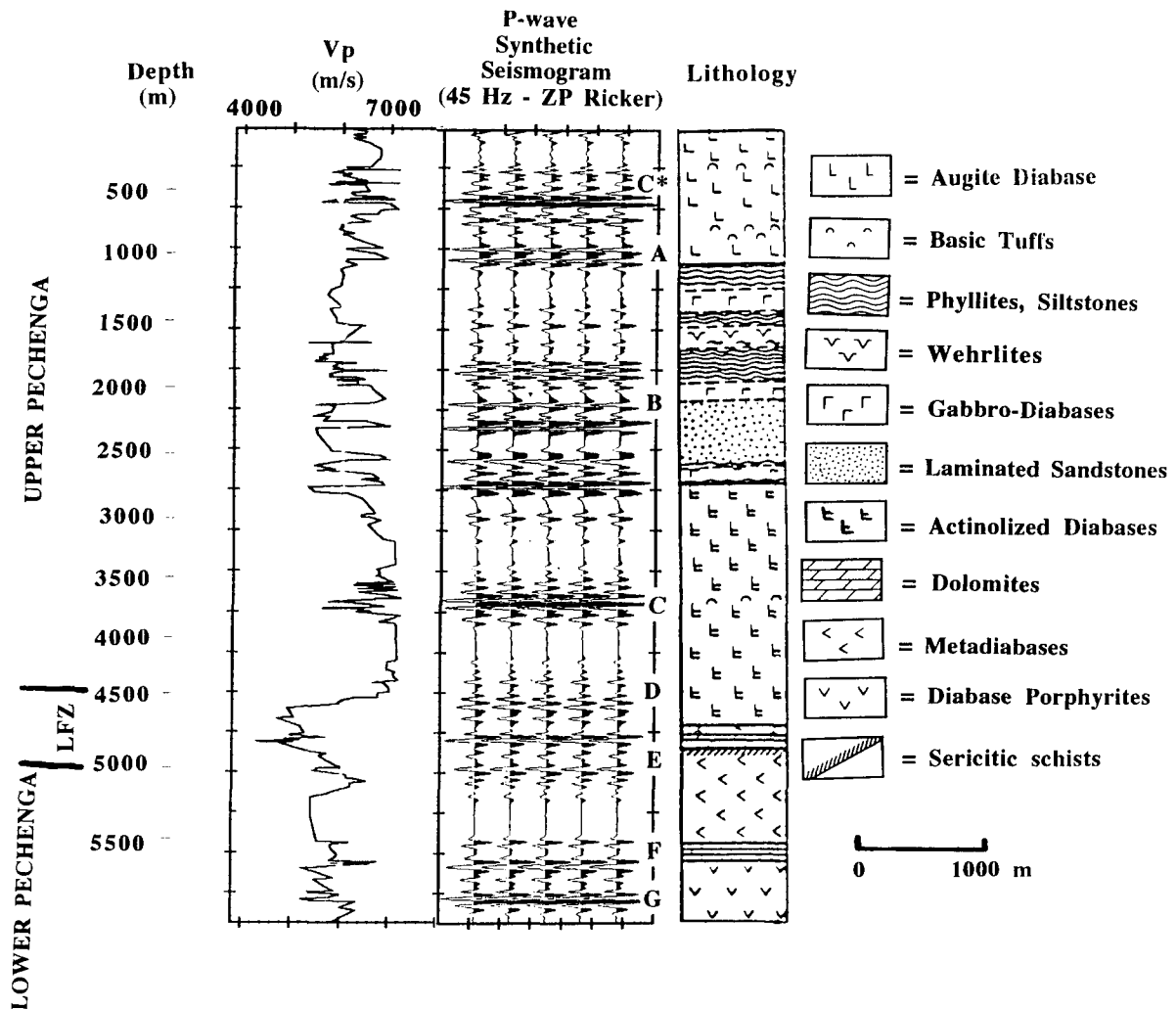


Fig. 3. 1-D P-wave synthetic seismogram (repeated 5 times) generated with a 45-Hz, zero-phase (ZP) Ricker wavelet. Shown with the velocity log and the generalized lithologies of the SG-3 borehole (modified from Lanev et al., 1987). C*, A–G refer to P-wave reflecting intervals, see text for details.

The Luchlompol major fault zone (LFZ) constitutes a distinct change from massive lavas to cataclasites and mylonites. This initially occurs at a depth of 4340 m, and continues to ~5100 m in the SG-3 borehole (Fig. 2). The LFZ is identified by foliated and mylonitized rocks, an increase in borehole cavernosity, a local increase in free water content, increasing temperature, and cataclastic fracturing (Kremenetsky and Krivtsov, 1991). As with the Lower Pechenga unit, this zone represents ductile deformation attributed to the Kola ocean closing (1.9 Ga) with associated alignment of mineral fabric. Lanev et al. (1987) reports that the foliations within the LFZ make an angle of 60–70° with core axes. The theoretical seismic response, at the LFZ, shows a well defined top (4673 m) and bottom (5050 m) reflection event (see D and E, Fig. 3). Additional events, between 4673 m and 5050 m in Fig. 3, represent the combination of amphibolite schists and metasedimentary rocks located in this zone.

The lower Proterozoic unit contains older andesitic basalts and minor clastic sequences that have been metamorphosed to epidote–amphibolite facies (Fig. 2). These lithologies tend to have lower densities (2.78–2.89 g cm⁻³), higher permeability and porosity, and lower P-wave velocities (6.0–6.4 km/s) (Pavlenkova, 1991). Foliation in metavolcanic zones is strongly developed and tends to be inclined 70–80° to core axes (Lanev et al., 1987; Vernik et al., 1994). Compared to the upper Pechenga unit, fewer gabbro and gabbro–diabase intrusions are present. Seismic synthetic reflectivity (Fig. 3) from this zone shows events that again correlate to interfaces consisting of actinolized diabase with: (1) metasedimentary rocks at ~5725 m (F); and (2) gabbroic–diabase at ~5800 m (G).

3. Acquisition and processing

The 1992 Kola VSP experiment was a multi-offset survey with the source locations at 200 m and 2080 m along S35°W and N11°E from SG-3, respectively (marked VSP-1 and VSP-2 in Fig. 4). These source locations are approximately parallel to the dip direction of the Pechenga structure and lie structurally down-dip and up-dip of the borehole.

Sources consisted of three compressional vibrators sweeping eight times per recording position in

the borehole with a 20-s linear upsweep from 15 to 90 Hz. The uncorrelated VSP data consist of 30-s records acquired every 25 m from 2175 to 6000 m in the SG-3 borehole using a four-component sonde (see Gal'perin, 1984). The sonde contains one vertically aligned geophone and three geophones at 126° from the vertical and equally spaced azimuthally about 360° (relative to the tool axis). The sonde was not equipped with orientation instrumentation so geophone alignment between each depth level was achieved by a four-component tool correction (see explanation later in this section). Since the SG-3 borehole has a maximum deviation of 10° at 6000 m, the vertical axis of the tool and the borehole coincide throughout the recorded depth range.

VSP data were also recorded in a satellite borehole (referred to as the sputnik borehole, Fig. 4) from 25 m to 525 m with the same tool and recording pa-

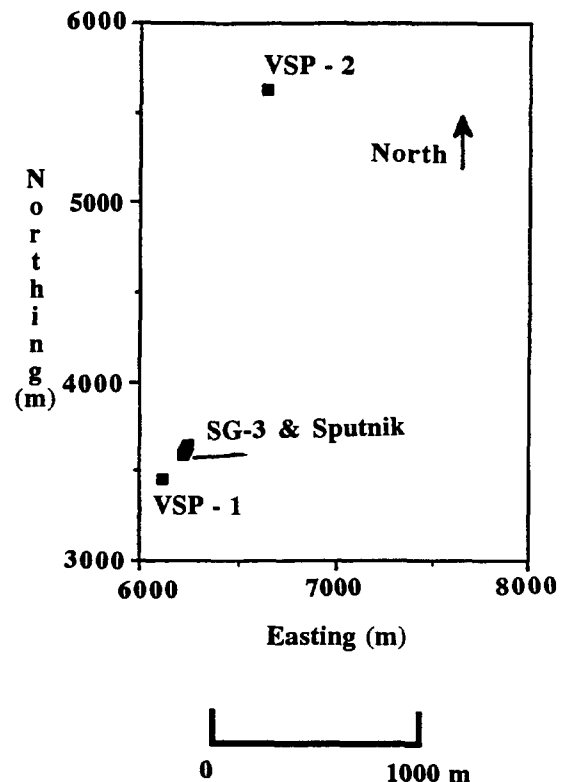


Fig. 4. Kola source locations for the 1992 VSPs. VSP-1 and VSP-2 were recorded in the SG-3 borehole from 2175 to 6000 m and the Sputnik borehole from 25 to 525 m.

Table 1
Processing sequence for the Kola VSPs

1	Preliminary cross-correlation for editing of bad data and intervals of tool sliding.
2	Diversity stack of the uncorrelated field data.
3	Cross-correlate the data with recorded Vibroseis sweep and extend the correlation to 20 s of listen time.
4	Organize the data by source location and component.
5	Geophone dephasing correction.
6	Signal-noise (F-X) filtering.
7	F-k filtering of slow velocities, e.g. tube wave.
8	Wavelet shaping deconvolution.
9	Four-component-based tool correction (output is in standard cartesian coordinate system).
10	Wavefield separation by median filtering.
11	P- and S- separation filtering, after Dankbaar (1987), on unseparated data followed by median filtering.
12	Display plots (500 ms AGC, biased amplitudes – 1.5x data RMS).
13	Pick direct and reflected apparent velocities of seismic phases: (a) elastic finite difference and ray trace modelling to determine seismic reflection behavior and apparent velocities; (b) calculate interval velocities from direct arrival P- and S-wave arrivals over 150-m increments (based on method described by Rühl and Hanitzsch, 1992); (c) calculate V_p/V_s ratio curves with average and interval velocities.

rameters. The sputnik VSP data, from VSP-1 and VSP-2, are displayed with the SG-3 data since the two boreholes are ~50 m apart. Although not indicated, four additional sputnik VSP source locations were recorded providing a unique opportunity to azimuthally analyze the near-surface seismic wavefield surrounding the SG-3 borehole, but will be presented in a future publication.

The processing of the VSP data followed a conventional scheme for crustal seismic data (Table 1) with two notable additions: (1) four-component tool corrections; and (2) P-S separation filtering (Dankbaar, 1987). Due to the fact that a sonde will rotate as it is raised to a new recording depth, it is necessary to collect tool orientation information from directional instruments on the tool, or infer the tool orientation based on the amount of a particular seismic phase which is recorded on each individual component. Because the recording tool used during the 1992 Kola VSPs did not have directional instrumentation, the direction and angle of incoming seismic energy (the source vector) was determined from the four-components by amplitude analysis of the direct P-wave (following a method originally described by DiSiena et al., 1984) and subsequently projected onto a cartesian coordinate frame. Traditionally for VSP recording, the in-line horizontal component (X) is assumed to be the largest horizontal amplitude. Therefore, at each depth level of the SG-3 recording, the projected horizontal components

were rotated so that the maximum power would lie along the in-line or X-direction.

Because of the dipping Pechenga structure (20–50°), P- and S-wave energy can be recorded on all components with varying amplitude strengths. Thus, P-S separation filtering (Dankbaar, 1987) was implemented to isolate the P- and S-wave energy from the unseparated vertical and unseparated in-line VSP recording directions. The filtering uses wireline sonic velocities as filter parameters in frequency-wavenumber space to distinguish P- and S-wave energy. Therefore, the resulting output consists of the P-wave response and S-wave response for the particular VSP and no longer strictly represents a distinct recording direction. Mode conversions are also filtered with this scheme and are output with the corresponding primary seismic phase (e.g., PS mode conversions are visible with the S-wave response).

4. The seismic wavefield in the 1992 Kola VSPs

The Kola VSPs highlight many primary and mode-converted seismic interfaces in addition to an ~6% decrease in apparent velocity beginning at ~4500 m depth. A typical data example is provided by the vertical component from VSP-1 (Fig. 5). Seismic boundaries can be initially identified from SP transmissions and P-wave reflections in this display. SP transmissions originate from 1200 m, 2600–2800 m, 3800 m, 4500 m, and 5100 m (Sp* on Fig. 4)

depths in the SG-3 borehole. Despite the interference from mode-conversions, two phases of reflection energy are recognizable in Fig. 5 by the negative slopes (apparent velocities) visible on the display. Elastic finite-difference forward modelling (2.5D) established that these reflections represent P- and S-waves from the dipping Pechenga sequences. P-wave reflections are distinguishable on VSP-1 Z at 2800 m, 3200 m, 4500 m, 5200 m (P in Fig. 5). P-wave reflections also originate from below the recorded interval (6500 ± 50 m and 6900 ± 50 m depth). One shear wave reflection, from the LFZ, is indicated in Fig. 4 (S). Therefore, seismic interfaces are identifiable by mode-converted as well as primary seismic phases.

LFZ (Fig. 5) marks the Luchlompol fault zone and the 6% decrease in apparent velocity which is seen as a break in slope of the direct P- and S-wave arrivals. Currently, the reduced velocity is attributed to either: (1) fracturing which results in

an increased free pore fluid presence (Kremenetsky and Krivtsov, 1991; Kazansky, 1992); or (2) a bulk composition change in combination with velocity anisotropy caused by foliation (Vernik et al., 1994) and no pore fluid presence. Later, it will be shown that the 1992 VSPs support the notion of free fluid presence based on V_p/V_s anomalies that are present at depths which reported free pore fluid presence when initially drilled.

Reflected P- and S-wave data are shown after median filtering and P-S separation filtering for the data from VSP-1 (Fig. 6a, b) and VSP-2 (Fig. 7a, b). P-wave and mode-converted P- to S-wave (PS) reflections delineate seismic boundaries at depths of 250 m, 1200 m, 1900 m, 2600–2800 m, 3200 m, 4500 m, 5100 m, and 5800 m (P in Fig. 6a and Fig. 7a; Ps in Fig. 6b and Fig. 7b). Reflections in the zone between 1900 m and 2800 m (Fig. 6a) represent boundaries of diabase intrusions and metasedimentary units of the upper Pechenga unit. Shear wave

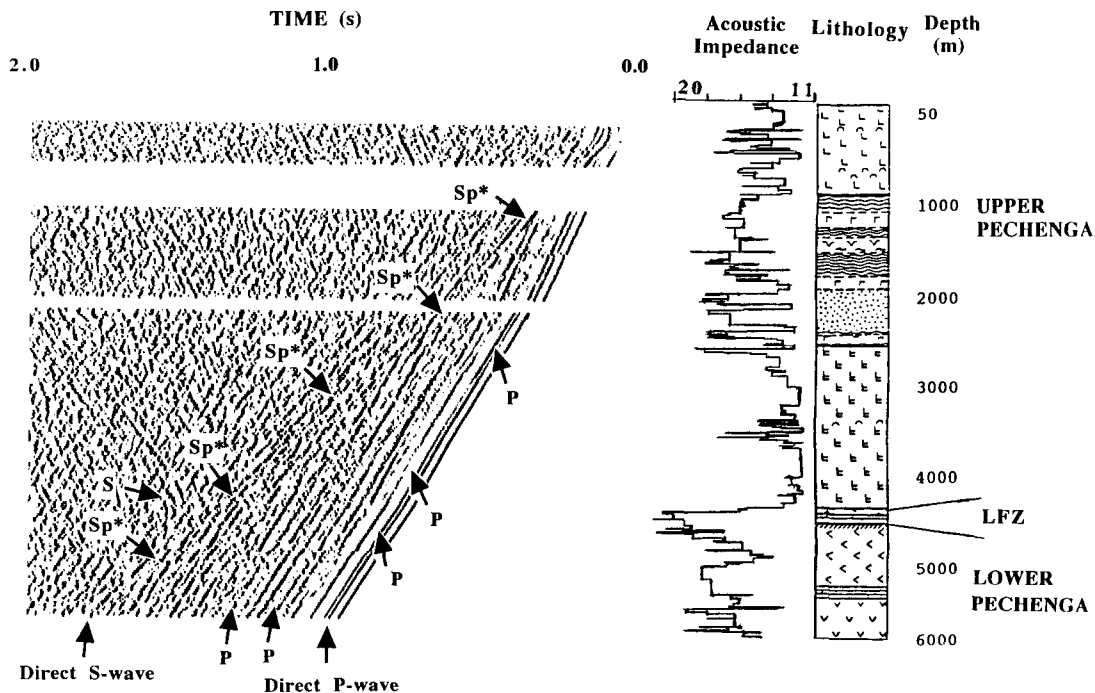


Fig. 5. Vertical component recording for Kola VSP-1 shown with the acoustic impedance curve ($(g \text{ s}^{-1} \text{ cm}^{-2})/10^4$) and generalized lithologies of the SG-3 borehole (data from 1200 to 2000 m are explosive data). Sp^* marks S- to P-wave transmitted energy. P refers to P-wave reflections in the data, and S illustrates an S-wave reflection. LFZ corresponds to the Luchlompol fault zone. Refer to Fig. 2 for lithologic symbol legend. Data shown with 500 ms AGC, and biased amplitudes ($1.5 \times$ data RMS).

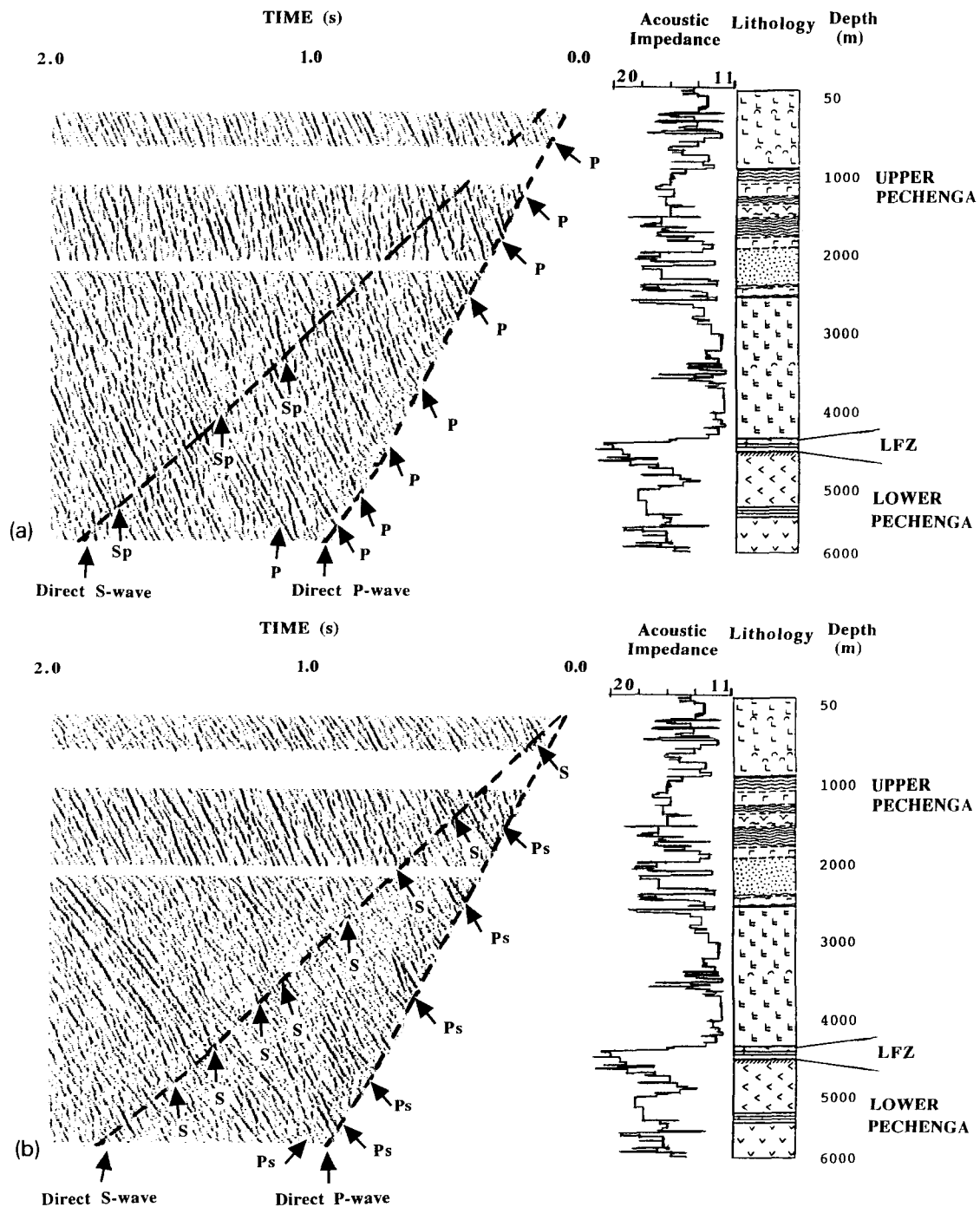


Fig. 6. (a) P-wave reflected wavefield after P-S separation filtering (Dankbaar, 1987) for VSP-1. The data are displayed with the acoustic impedance curve and lithologic section (units the same as Fig. 5). *P* represents P-wave reflections; *Sp* marks S- to P-wave mode-converted reflection. The dashed lines indicate the positions of the direct P- and S-waves. Data displayed with same parameters as Fig. 5. (b) S-wave reflected wavefield after P-S separation filtering (Dankbaar, 1987) for VSP-1 with the acoustic impedance curve and lithologic section (units the same as Fig. 5). *Ps* = P- to S-wave mode-converted reflections; *S* = S-wave reflections. The dashed lines indicate the positions of the direct P- and S-waves. Data displayed with same parameters as Fig. 5.

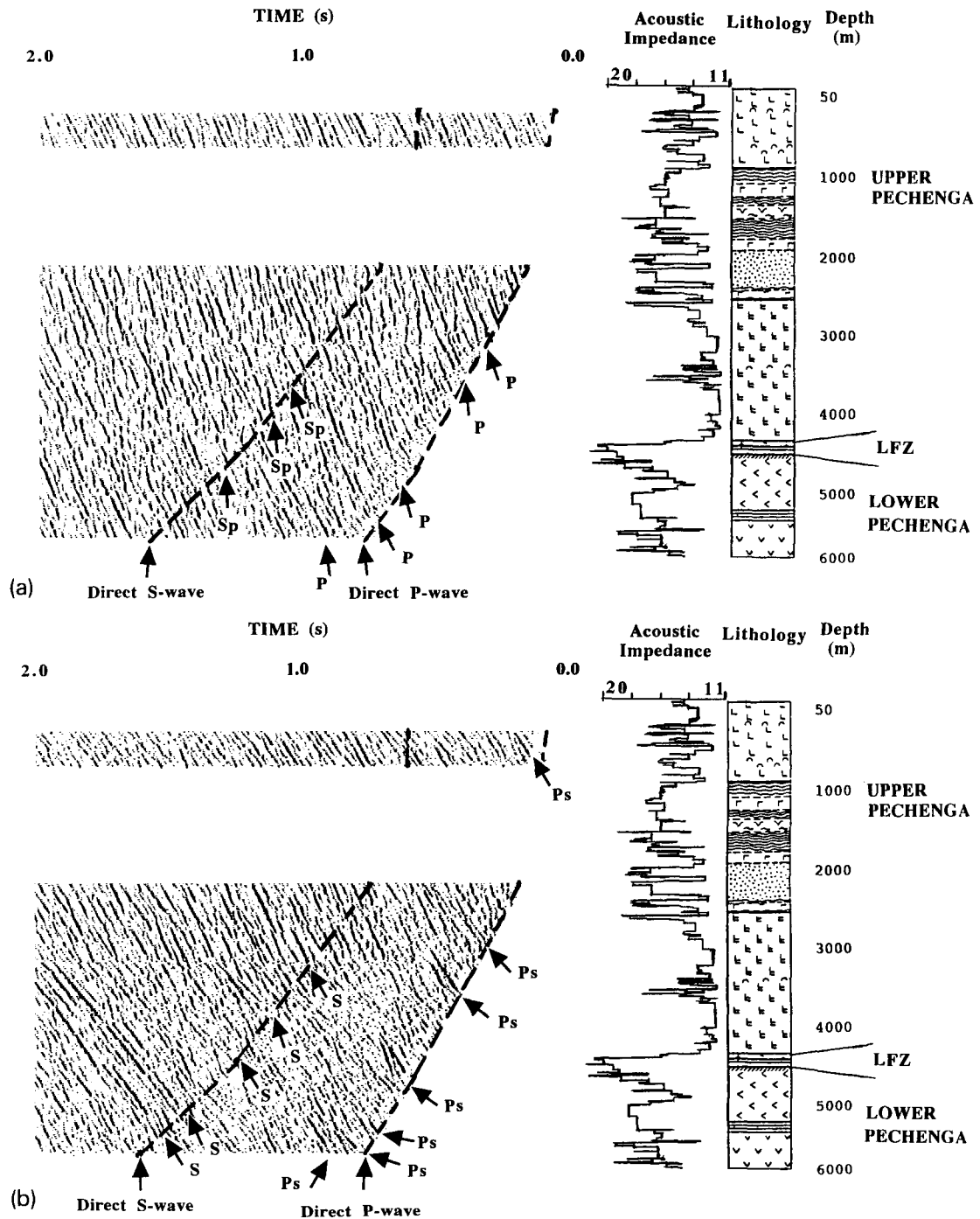


Fig. 7. (a) P-wave reflected wavefield after P-S separation filtering (Dankbaar, 1987) for VSP-2. The data are displayed with the acoustic impedance curve and lithologic section (units the same as Fig. 5). *P* represents P-wave reflections; *Sp* marks S- to P-wave mode-converted reflection. The dashed lines indicate the positions of the direct P- and S-waves. Data displayed with same parameters as Fig. 5. (b) S-wave reflected wavefield after P-S separation filtering (Dankbaar, 1987) for VSP-2 with the acoustic impedance curve and lithologic section (units the same as Fig. 5). *Ps* = P- to S-wave mode-converted reflections; *S* = S-wave reflections. The dashed lines indicate the positions of the direct P- and S-waves. Data displayed with same parameters as Fig. 5.

reflections (S in Fig. 6b and Fig. 7b) appear at the same levels except 1200 m, 6500 m, and 6900 m. S-waves reflections are identifiable at depths of 250 m, 1900 m, 2600 m, 3800 m, 4500 m, and 5100 m (the largest relative amplitudes occur at 1900 m, 3800 m, 4500 m and 5100 m). SP reflections occur at the 3800 m, 4500 m, and 5100 m depth levels (Sp in Fig. 6a, and Fig. 7a).

Although fewer reflections are identifiable on P–S filtered VSP-2 data (Fig. 7a, b), the same general observations about the depths of reflectivity are displayed. VSP-2 (Fig. 7b) displays better coherency for the PS reflected events than the primary P reflected phases (Fig. 7a). This results from the source being up-dip of the borehole (and offset) which forces the reflected energy to strike the borehole at angles between 35° and 55°. At these angles, mode-converted reflections have equivalent or greater amplitude than the corresponding primary phases (Tooley et al., 1965).

5. Discussion

The VSP-defined seismic boundaries, along the SG-3 borehole, are summarized in Fig. 8 with V_p/V_s curves (determined from VSP), bulk borehole stratigraphy and mapped shear zones. Along with the principal question regarding the causes of reflectivity in the Kola borehole, the VSPs will address the related issues of free pore fluid and subhorizontal reflectivity within the borehole sequences (observed on surface seismic data between 2.0 and 3.0 s TWT, see Mints et al., 1989 or Pavlenkova, 1991).

P-wave reflectivity in the Kola VSP is caused both by shear zones and lithologic interfaces. Occasionally, the depths of the shear zones and the lithologic contrasts coincide, likely enhancing the reflectivity from these depths. Mylonitic shear zones are known to be a source of crustal reflectivity (Hurich et al., 1985). In the upper 6000 m of the Kola borehole sequence, mylonitic shear zones are mapped at depths corresponding to reflecting boundaries as shown in the VSP data (Fig. 8). The events at 250 m, and 3800 m are diabase intrusions within the larger metatuffaceous sequences. The reflections from 5800 m mark ~100 m of metasedimentary units that correspond to the base of the Kuvernerinyok suite of dolomitic marls, and quartzites. Immediately

below the recorded interval at 6500 ± 50 m, the reflectivity is generated at the base of a sequence of gabbro–diabases intruded into biotite–amphibole–plagioclase schists (Lanev et al., 1987). Finally, the event from 6900 ± 50 m is interpreted to be the Proterozoic–Archean interface at 6842 m which is composed of biotite–amphibole–plagioclase schists above biotite–plagioclase gneisses and schists with high aluminiferous minerals (Lanev et al., 1987).

Shear wave reflectivity is similar to that of the P-waves, except for large relative amplitude shear events which occur at 1900 m, 3800 m, 4500 m, and 5100 m. These depths define three mylonitic shear zones and one lithologic contact (1900 m). The lower intervals also correspond to depths of relative V_p/V_s increases (Fig. 8). Generally, an increase in the V_p/V_s ratio can be explained by a decrease in relative quartz content, or an increase in the amount of water present at those depths (Nur and Simmons, 1969). Evaluating relative quartz content percentages provided by Kremenetsky et al. (1987), a reduction in the quartz content is not significant at these depths. Therefore, the presence of fluids at these levels is possibly the cause of the V_p/V_s increases, which in turn marks a basic physical property change enhancing the shear wave reflectivity at these depths. Kremenetsky and Krivtsov (1991) provide additional support for this interpretation by reporting increased free fluid percentages at depths of 1900 m, 3800 m, 4500 m, and 5100 m.

The last seismic events of particular interest are the SP reflections present on both the VSP-1 and VSP-2 sections from 3800 m, 4500 m, and 5100 m. The SP reflection events are enhanced due to the structural dip. Zoeppritz equations predict that for angles of incidence as small as 20–25°, the SP reflection coefficient exceeds the S-wave reflection coefficient. Since these events appear at 3800 m, 4500 m and 5100 m, it is again possible that a pore fluid presence enhances the amplitude of these events by increasing the acoustic velocity contrast at these levels. Given the presence of these phases in the VSP data, it is possible that SP reflections could appear on a conventional P-wave surface stack section of the region (although the resulting image would be blurred due to incorrect normal moveout correction if apparent at all as discussed by Fertig and Krajewski, 1990). Additional work on the imaging potential of

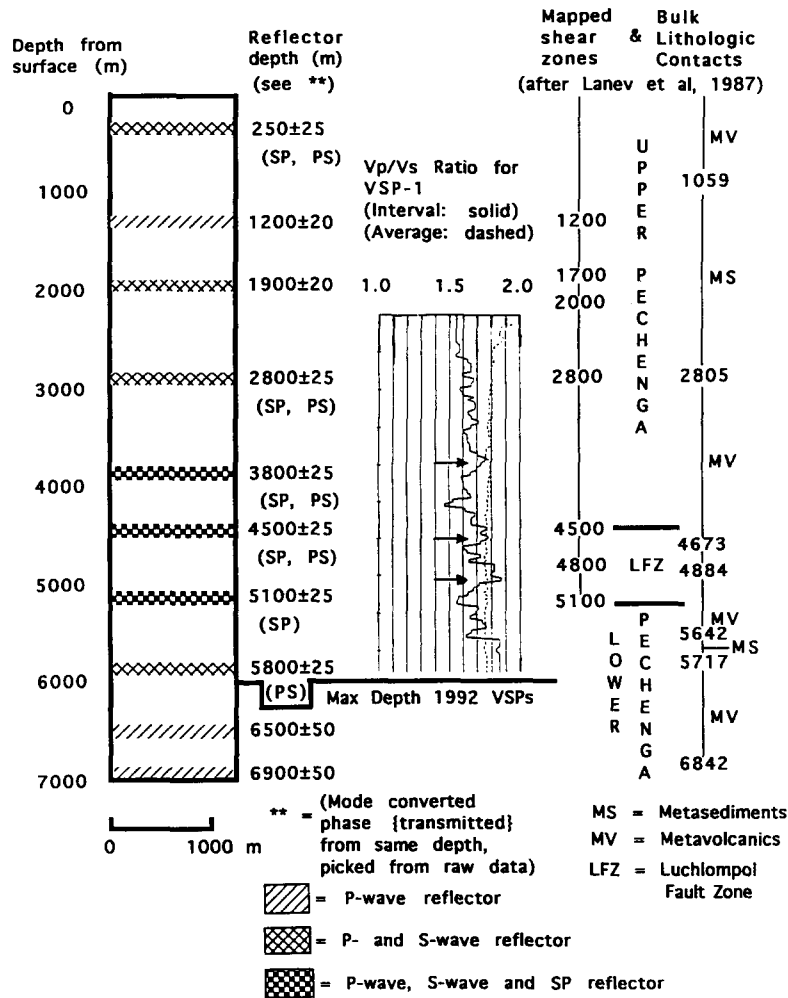


Fig. 8. Summary of seismic interfaces identified from the 1992 Kola VSPs. Depths to reflectors, mapped shear zones (after Kazansky, 1992), generalized lithologic contacts (after Lanev et al., 1987), and depths to mode-converted transmissions are identified. The recorded depth range is from 0 to 6000 m, so deeper reflectors (6500 m, and 6900 m) are interpreted from analysis of deeper reflection events. V_p/V_s ratio curves (calculated from average (dashed line) and interval (solid line) velocities for VSP-1 from 2175 to 6000 m) are also shown. Three zones of increased V_p/V_s are noted by the arrows. The interval velocities were determined after the method described by Rühl and Hanitzch (1992) with a 150-m depth window. Note: error bars determined as \pm one depth sampling interval (25 m) on reflector depth, and a maximum of ± 0.05 (based on Gaussian error propagation method) for the interval V_p/V_s curve.

SP energy is discussed by Frasier and Winterstein, 1990.

Subhorizontal reflectivity is interpreted in the Kola region on CMP sections from ~4500 m to 9000 m where foliations still dip at 30° or greater (Mints et al., 1989; Pavlenkova, 1991; I. Ganchine, pers. commun., 1995). Currently, two hypotheses exist for the presence of these events. Mints et al. (1989) at-

tributes these events to subhorizontal shearing below the Proterozoic complex based on increased microcrack porosity at depth from SG-3 core. Vernik et al. (1994) argue that the increased microcrack porosity is a result of core damage upon recovery and not a viable explanation of the horizontal events. They propose that the subhorizontal reflections are amphibolite intrusions, especially between 7500 m

and 9000 m. Unfortunately, the 1992 VSPs do not sample this zone and show no distinct indication of horizontal reflectivity between 4500 m and 6000 m. Yet, the vertical component (Fig. 5) and separated P-wave data (Fig. 6a, and Fig. 7a) both contain SP reflections, as previously discussed. Therefore, the subhorizontal reflectivity, within zones of dipping geology on CMP sections, may represent partial stacking of SP phases. Elastic finite-difference modelling of these events, for both the Kola VSP and surface recording geometry's, support this idea and will be fully presented in a future publication.

6. Conclusions

The 1992 Kola VSPs show an abundance of reflections and mode conversions in Precambrian crystalline sequences which dip 20–50° and vary in metamorphic grade. The Kola VSPs also highlight a 6% velocity decrease which coincides to the Luchlompol major fault zone (a mylonitic shear zone between 4500 m and 5100 m depths within the SG-3 borehole).

P-wave reflectivity in the recorded borehole section is dominated by mylonitic shear zones (1200 m, 1900 m, 2800 m, 4500 m, and 5100 m) and lithologic contrasts (diabase within a metatuff: 250 m, and 3800 m; metavolcanic–metasedimentary contacts: 1900 m, 2800 m, and 5800 m). S-wave reflectivity coincides with the P-wave interfaces except at 1200 m (a mylonite zone), and the two reflectors below 6000 m (~6500 m: contact between gabbro–diabase and biotite schists; and ~6900 m: contact of biotite schists and biotite gneisses).

S-wave reflections show relative amplitude increases at zones where a mappable increase in water content was reported during initial drilling (1900 m, 3800 m, 4500 m, and 5100 m), and correspond to V_p/V_s ratio increases determined from VSP interval velocity calculations. The presence of free pore fluid is inferred at zones of sharp increase in the V_p/V_s ratio (3800 m, 4500 m and 5100 m depths) since decreased quartz content is not reported to be significant at these depths. The enhanced impedance contrast, possibly due to free pore fluid presence, increases the relative amplitudes for S-wave and SP reflection phases and these depths.

SP mode-converted reflections are also recorded on both the vertically incident (VSP-1) and offset

(VSP-2) VSPs at 3800 m, 4500 m and 5100 m depth, and result from a combination of dipping structure, a 6–9% decrease in acoustic impedance, and probably an increase in relative percentage of water present.

Acknowledgements

This work was supported by NSF grant EAR-9118600. The authors would like to thank Dr. M. Lizinski of the St. Petersburg Mining Institute for providing access to the additional Russian VSP data, and the acoustic impedance curve for the Kola Superdeep Borehole. We wish to thank Dr. I. Morozov, I. Ganchine, and Dr. D. Ilynski for their work on various parts of the Kola seismic data. The principle author thanks Dr. R. Carbonell, Dr. A. Prugger, and Dr. Z. Hajnal for numerous discussions about this work. We also wish to thank D. White, E. Lüschen, and an anonymous reviewer for their helpful comments.

References

- Berthelsen, A. and Marker, M., 1986. Tectonics of the Kola Collision suture and adjacent Archean and early Proterozoic terrains in the Northeastern region of the Baltic Shield. *Tectonophysics*, 126: 31–55.
- Blundell, D.J. and Raynaud, B., 1986. Modeling lower crust reflections observed on BIRPS profiles. In: M. Barazangi and L. Brown (Editors), *Reflection Seismology—a global perspective*. Am. Geophys. Union Geodyn. Ser., 13: 287–297.
- Dankbaar, J.W.M., 1987. Vertical Seismic Profiling—separation of P- and S-waves. *Geophys. Prospecting*, 35: 803–814.
- DiSiena, J.P., Gaiser, J.E. and Corrigan, D., 1984. Horizontal component and shearwave analysis of three component VSP data. In: N.M. Töksoz and R.R. Stewart (Editors), *Vertical Seismic Profiling Part B: Advanced concepts*. Geophysical Press, Amsterdam, 14B, 177–188.
- Fertig, J. and Krajewski, P., 1990. Acquisition and processing of pure and converted shear waves generated by compressional wave sources. In: R. Marschall (Editor), *Aspects of Seismic Reflection Data Processing*. Kluwer Academic Publishers, The Hague, pp. 103–132.
- Fountain, D.M., Boundy, T.M., Austrheim, H. and Rey, P., 1994. Eclogite facies shear zones—Deep crustal reflectors?. *Tectonophysics*, 232: 411–424.
- Fountain, D.M., McDonough, D.T. and Gorham, J.M., 1987. Seismic reflection models of continental crust based on metamorphic terrains. *Geophys. J. R. Astron. Soc.*, 89: 61–67.
- Frasier, C. and Winterstein, D., 1990. Analysis of conventional and converted mode reflections at Putah sink, California using three-component data. *Geophysics*, 55: 646–659.
- Fuchs, K., 1969. On the properties of deep crustal reflections. *J. Geophys.*, 35: 133–149.

- Gal'perin, E.I., 1984. The Polarization Method of Seismic Exploration. B. Kuznetsov, M. Samokhvalov (Translators) D. Reidel Publishing Co., Dordrecht, 268 pp.
- Hale, L.D. and Thompson, G.A., 1982. The seismic reflection character of the Mohorovicic discontinuity. *J. Geophys. Res.*, 87: 4625–4635.
- Hohrath, A., Bram, K., Hanitzsch, C., Hubral, P., Kästner, U., Lüschen, E.; Rühl, T., Schrueth, P.K. and Söllner, W., 1992. Evaluation and interpretation of VSP-measurements in the KTB–Oberpfalz pilot borehole. *Sci. Drilling*, 3: 89–99.
- Hurich, C.A., Smithson, S.B., Fountain, D.M. and Humphreys, M.C., 1985. Seismic Evidence of mylonite reflectivity and deep structure in the Kettle Dome metamorphic core complex. *Geology*, 13: 577–580.
- Juhlin, C. and Windhofer, M., 1988. Interpretation of the seismic reflectors in the Gravberg-1 Well. In: A. Boden and K.G. Erickson (Editors), *Deep Drilling in Crystalline Bedrock*. Springer-Verlag, Berlin, pp. 113–121.
- Kazansky, V.I., 1992. Deep structure and metallogeny of Early Proterozoic mobile belts in light of superdeep drilling in Russia. *Precambrian Res.*, 58: 289–303.
- Kazansky, V.I., Smirnov, Y.P. and Kuznetsov, Y.I., 1987. Shear zones and mineralized fissures. In: Y.A. Koslovsky (Editor), *The Superdeep Well of the Kola Peninsula*. Springer-Verlag, Berlin, pp. 223–240.
- Koslovsky, Y.A. (Editor), 1987. *The Superdeep Well of the Kola Peninsula*. Springer-Verlag, Berlin, 558 pp.
- Kremenetsky, A.A. and Krivtsov, A.I., 1991. Models and cross-sections of the Earth's crust-based on superdeep drilling data of the USSR. Ministry of Geology of the USSR. Moscow, Publication 164.
- Kremenetsky, A.A., Ovchinnikov, L.N., Banshchikova, I.V., Lapidus, I.V. and Rusanov, M.S., 1987. Geochemistry and conditions of formation of the Precambrian complexes. In: Y.A. Koslovsky (Editor), *The Superdeep Well of the Kola Peninsula*. Springer-Verlag, Berlin, pp. 113–165.
- Lanev, V.S., Nalivkina, E.B., Vakhrusheva, V.V., Golenkina, E.A., Rusanov, M.S., Smirnov, Y.P., Suslova, S.N., Duk, G.G., Koltsova, T.V., Maslennikov, V.A., Timofeev, B.V. and Zaslavsky, V.G., 1987. Geological section of the well. In: Y.A. Koslovsky (Editor), *The Superdeep Well of the Kola Peninsula*. Springer-Verlag, Berlin, pp. 40–73.
- Levander, A., Hobbs, R.W., Smith, S.K., England, R.W., Synder, D.B. and Holliger, K., 1994. The crust as a heterogeneous 'optical' medium, or 'crocodiles in the mist'. *Tectonophysics*, 232: 281–297.
- Lüschen, E., Bram, K., Söllner, W. and Sobolev, S., 1996. Nature of seismic reflections and velocities from VSP-experiments and borehole measurements at the KTB deep drilling site in southeast Germany. In: D.J. White, J. Ansorge, T.J. Bodoky and Z. Hajnal (Editors), *Seismic Reflection Probing of the Continents and Their Margins*. *Tectonophysics*, 264(1–4): 309–326 (this volume).
- Mints, M.V., Kolpakov, N.I., Lanev, V.S. and Rusanov, M.S., 1989. The character of the subhorizontal seismic boundaries within the upper part of the Earth's crust (according to data from the Kola Ultradeep Well). *Geotectonics*, 21: 444–451.
- Mooney, W.D. and Meissner, R., 1992. Multi-genetic origin of crustal reflectivity: a review of seismic reflection profiling of the continental lower crust and Moho. In: D.M. Fountain, R. Arculus and R.W. Kay (Editors), *Continental Lower Crust—Developments in Geotectonics*, 23. Elsevier, Amsterdam, pp. 45–80.
- Nur, A. and Simmons, G., 1969. The effect of saturation on velocity in low porosity rocks. *Earth Planet. Sci. Lett.*, 7: 183–193.
- Pavlenkova, N.I., 1991. The Kola superdeep drillhole and the nature of seismic boundaries. *Terra Nova*, 4: 117–123.
- Rector, J.W., 1988. Acquisition and Preliminary analysis of oriented multicomponent multi-offset VSP data: DOSECC Cajon Pass Deep Scientific Drillhole. *Geophys. Res. Lett.*, 15: 1061–1064.
- Rühl, T. and Hanitzsch, C., 1992. Average and interval velocities derived from first breaks of vertical seismic profiles at the KTB pilot hole. *KTB Rep. 92-5*: 201–220.
- Smithson, S.B., Shive, P.N. and Brown, S.K., 1977. Seismic reflections from Precambrian crust. *Earth Planet. Sci. Lett.*, 37: 333–338.
- Smithson, S.B. and Johnson, R.A., 1989. Crustal structure of the western U.S. based on reflection seismology. In: L.C. Pakiser and W.D. Mooney (Editors), *Geophysical Framework of the Continental United States*. *Geol. Soc. Am. Mem.*, 172: 577–612.
- Söllner, W., Lüschen, E., Li, X.P., Hubral, P., Gut, T.W. and Widmaier, M., 1992. VSP—A Link between Reflection Seismic Profiling and Lithology. *KTB Rep. 92-5*: 169–200.
- Steinhart, J.S. and Meyer, R.P., 1961. *Exploratory Studies of Continental Structure*. Carnegie Institute of Washington, 622, 409 pp.
- Tooley, R.D., Spencer, T.W. and Sagoci, H.F., 1965. Reflection and transmission of plane compressional waves. *Geophysics*, 30: 552–570.
- Valasek, P.A., Snoke, A.W., Hurich, C.A. and Smithson, S.B., 1989. Nature and origin of seismic reflection fabric, Ruby–East Humboldt metamorphic core complex, Nevada. *Tectonics*, 8: 391–415.
- Vernik, L., Hickman, S., Lockner, D. and Rusanov, M., 1994. Ultrasonic velocities in cores from the Kola Superdeep well and the nature of subhorizontal seismic reflections. *J. Geophys. Res.*, 99: 24209–24219.